A novel and affordable DCE-MRI phantom: Prospective assessment of DCE-MRI breast protocols

Araminta E. W. Ledger[1], Marco Borri[1], Hector Sanchez Casas[1], Craig Cummings[1], Maria A. Schmidt[1], and Martin O. Leach[1]

[1]*CR-UK and EPSRC Cancer Imaging Centre, The Institute of Cancer Research and Royal Marsden NHS Foundation Trust, Sutton, Surrey, United Kingdom*

Introduction

T1-weighted dynamic contrast-enhanced (DCE) MRI breast sequences are a well-established component of breast MRI screening protocols. However, although international guidelines provide standardized recommendations [1], the wide array of possible sequence parameters results in a broad range of compliant sequences. These sequence differences can produce contrast agent (CA) enhancement curves with variable screening sensitivity [2]. Although standard test objects can be used to verify the dependence of image intensity on CA concentration, it is very difficult to prospectively assess the impact of common sequence parameter changes on CA uptake curves. This work used a novel test object, able to create reproducible CA enhancement curves, to prospectively evaluate the effect of common protocol alterations on two clinical breast protocols.

Materials and Methods

MRI Protocols: Two current clinical breast DCE-MRI protocols, performed with 3D fat-suppressed spoiled gradient-echo sequences, were selected for evaluation (Protocol 1: Siemens Aera 1.5T; Protocol 2: Philips Achieva 3.0T; see Table 1). Each dynamic series consisted of one pre-contrast and eight post-contrast axial images with CA (DOTAREM; Guerbet, France) administered at the end of the pre-contrast image.

Experimental Set-Up: The test-object consists of a 40 mm inside-diameter (ID) sphere divided into four inter-linking compartments with a liquid input and output (each 3 mm ID) (see Figure 1). The input was connected to an automated clinical injector (MedRad, USA) and a standardised procedure for injection of water and CA was adopted: [i] 8 mL water at 0.14 mL/s; [ii] 2 mL of 0.05 mM CA at 0.5 mL/s; [iii] 72 mL water at 0.14 mL/s ensuring that CA was injected following the first dynamic image acquisition. The signal intensity of each image was evaluated from a rectangular region of interest (ROI) placed on the output (see Figure 1): the dilution of CA within the sphere modifies the input CA concentration curve, resulting in a CA enhancement curve with wash-out characteristics [3]. In a separate reproducibility study at high temporal resolution (3.3s), variability was measured at ±3% at peak enhancement.

Sequence Investigation: Two sequence alterations were selected for investigation: CA injection timing and k-space sampling pattern. (i) For each protocol, CA was injected at 15s and then 30s earlier; (ii) A motion compensation strategy was applied to each protocol whilst maintaining the length of the dynamic sequence. Protocol 1 was altered to a random k-space sampling pattern (dynamic acquisition = 56.6s) whilst radial sampling was applied to Protocol 2 (dynamic acquisition = 55.7s).

Data Analysis: Relative enhancement (RE) (percentage increase of signal intensity: $([SI - SI_{pre\text{-}contrast}]/SI_{pre\text{-}contrast} \times 100)$ was calculated for each dynamic sequence from the signal intensity of the output ROI. Baseline repeatability was assessed for each clinical breast protocol from three subsequent dynamic acquisitions, and expressed as the relative standard deviations (%RSD) at peak and final relative enhancement (see Table 2). Test-retest repeatability was evaluated on Protocol 1 on two separate occasions under the same experimental conditions (see Figure 2).

Table 1: Clinical breast protocols

Protocol	1	2
No. slices	160	170
Repetition time [TR, ms]	4.50	4.54
Echo time [TE, ms]	2.00	2.19
Flip angle [°]	18	16
Slice thickness [mm]	1.0	1.0
In-plane resolution [mm]	1.3	1.0
Acquisition length [s]	56.3	55.2
K-space sampling scheme	Half-Fourier	Linear
Centre of k-space [s]	19.5	29.8

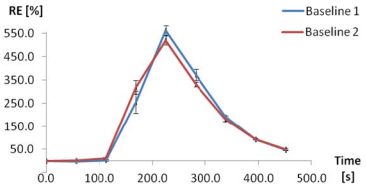

Figure 2: Baseline RE measurements obtained from Protocol 1 on two separate occasions under the same experimental conditions. Error bars represent standard deviation.

Figure 1: DCE-MRI test object set up within breast coil, showing test object and outlet (dotted and plain arrows). ***Inset:*** Four compartments within the test object.

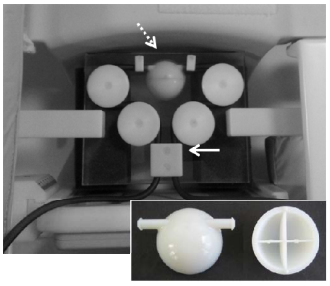

Table 2: Baseline Repeatability

Protocol	Peak RE [%]		Final RE [%]	
	Mean ± SD	%RSD	Mean ± SD	%RSD
1 (1)	520.8 ± 18.5	± 3.6	51.0 ± 4.6	± 9.0
1 (2)	562.3 ± 20.4	±3.6	46.9 ± 0.8	±1.8
2	408.1 ± 29.6	±7.3	34.9 ± 1.4	±8.0

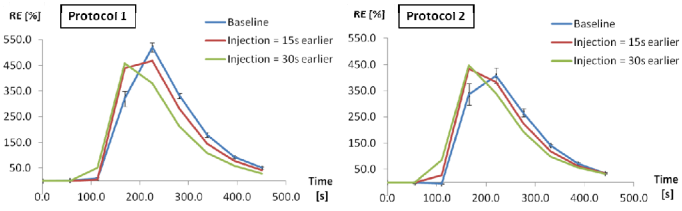

Figure 3: RE curves resulting after advanced CA injection (15 and 30s) against baseline RE curves (error bars represent standard deviation) for Protocols 1 and 2, respectively.

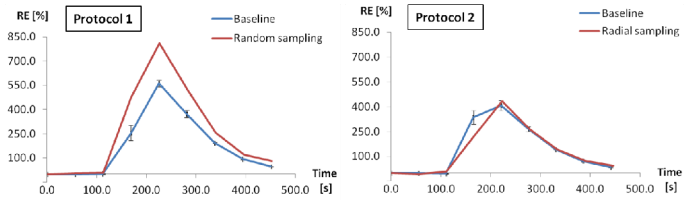

Figure 4: RE curves resulting from k-space sampling alteration against baseline RE curves (error bars represent standard deviation) for Protocol 1 and 2, respectively.

Results & Discussion

Baseline Repeatability: Table 2 displays the mean measures of peak and final RE together with relative standard deviation (%RSD) for the baseline experiments. For each protocol, the RE curves produced by the test object achieved good baseline repeatability (see Table 2). Test-retest repeatability was also measured: Figure 2 plots the baseline RE curves obtained from Protocol 1 in two separate experiments (SD at each dynamic baseline measurement is displayed). Following protocol alterations, any difference in the RE curves beyond these SD limits was considered to be significant.

Sequence Alteration: Figure 3 displays the RE curves obtained from the earlier CA injection timings (15 & 30s) against the baseline RE curve measurement for Protocols 1 and 2, respectively. In each case, shortening the lead-in time prior to CA injection significantly altered the RE curves obtained. For Protocol 1, the earlier injection times resulted in earlier enhancement but with a concomitant reduction in peak RE (520.8% to 468.0%, respectively) – the centre of k-space acquisition for the pertinent dynamic images was no longer coincident with the peak CA concentration. However, for Protocol 2 (k-space centre = 29.8s), reducing the injection lead-in by 30s more closely aligned the k-space centre acquisition with peak CA concentration resulting in earlier enhancement and greater peak RE (408.1% to 446.4%, respectively). Figure 4 displays the RE curves obtained from the alteration of k-space sampling pattern. The random k-space sampling pattern resulted in a significant increase in peak RE from 562.3% to 810.4% for Protocol 1, whilst the application of radial k-space sampling to Protocol 2 resulted in a sharper curve shape but with no significant difference in peak RE (408.1% to 435.2%).

Conclusions: Test object repeatability was established at low temporal resolution and enabled the prospective evaluation of common sequence alterations on two breast DCE-MRI protocols. None of the above protocol alterations resulted in the risk of enhancement curve misclassification, indicating robust sequences. However, CA injection should be timed to align peak CA concentration with the centre of k-space acquisition in order to maximise peak RE. In addition, k-space sampling scheme should be carefully considered as sampling strategies can impact on enhancement curve characteristics. Sequence comparison with this test object can help to establish robust DCE-MRI breast protocols and provides a useful addition to standard quality assurance practice.

References: [1] Breast MRI Accreditation Program Requirements; ACR 2012:1–16; [2] Jansen *et al.*; Am J Roentgenol 2009;193(3):832–9; [3] Kuhl *et al.*; Radiology 1999; 211; 101-110. **Acknowledgements**: We acknowledge the support received for the CRUK and EPSRC Cancer Imaging Centre in association with the MRC and Department of Health (England) (grant C1060/A10334), NIHR funding to the Clinical Research Facility in Imaging and the Biomedical Research Centre, the Technology Strategy Board (grant M1550J) and an NIHR Transitional Research Fellowship (TRF-2013-06-003).